Spironolactone Prevents Diabetic Nephropathy through an Anti-Inflammatory Mechanism in Type 2 Diabetic Rats

Sang-Youb Han,*† Cy-Hyun Kim,† Han-Seong Kim,‡ Yi-Hwa Jee,§ Hye-Kyoung Song,§ Mi-Hwa Lee,§ Kum-Hyun Han,§ Hyoung-Kyu Kim,§ Young-Sun Kang,§ Jee-Young Han,‖ Young-Sik Kim,¶ and Dae-Ryong Cha§

**Department of Internal Medicine, †Clinical Research Center, and ‡Department of Pathology, Inje University, Ilsan-Gu, Goyang City, and Departments of §Internal Medicine and ¶Pathology, Korea University, Ansan City, Kyungki-Do, and ‖Department of Pathology, Inha University, Chung-Gu, Sinheung-dong, Chung-Gu, Incheon, Korea*

Aldosterone induces myocardial fibrosis and vascular inflammation *via* proinflammatory and profibrotic cytokines. The effect of spironolactone on renal inflammation and renal function was investigated in type 2 diabetic rats. For define the molecular mechanism of spironolactone, the effect of spironolactone on the synthesis of monocyte chemotactic peptide-1 (MCP-1) and its upstream transcription factor, NF-κB, was evaluated in cultured mesangial cells and proximal tubular cells. There were no changes in blood glucose concentration or BP after spironolactone treatment. Spironolactone treatment significantly reduced urinary albumin excretion and ameliorated glomerulosclerosis. Urinary levels of MCP-1 were significantly increased concurrently with renal expression of MCP-1, macrophage migration inhibitory factor, and macrophage infiltration. Spironolactone treatment significantly inhibited urinary excretion of MCP-1 as well as renal MCP-1 and migration inhibitory factor expression and macrophage infiltration. In addition, aldosterone induced upregulation of MCP-1 expression and NF-κB transcriptional activity in cultured cells, and spironolactone reduced both NF-κB activation and MCP-1 synthesis. Furthermore, NF-κB inhibition abolished aldosterone-induced MCP-1 production. Overall, these findings suggest that aldosterone-induced NF-κB activation leads to activation of proinflammatory cytokines, ultimately leading to renal injury in this model. These data suggest that mineralocorticoid blockade may be a potential therapeutic target in diabetic nephropathy.

J Am Soc Nephrol 17: 1362–1372, 2006. doi: 10.1681/ASN.2005111196

Although diabetic nephropathy has not been considered to be an immune-mediated renal disorder, an inflammatory mechanism has been suggested to be contributing to the pathogenesis of diabetic nephropathy (1–3). Anti-inflammatory agents, such as mycophenolate mofetil and retinoic acid, prevent the development of glomerular injury in streptozotocin-induced diabetic rats (4,5). In addition, macrophage accumulation and activation in the kidney have been correlated with albuminuria and renal fibrosis (6). Taken together, these findings suggest that anti-inflammatory agents might prevent renal disease progression in diabetic nephropathy.

Aldosterone causes direct myocardial fibrosis and inflammatory reactions, as well as left ventricular hypertrophy (7,8). The more direct evidence of aldosterone as a potential mediator of tissue injury came from study results that showed that aldosterone caused vascular and renal injury in the presence of angiotensin-converting enzyme inhibition and that aldosterone antagonism resulted in marked vascular protection, even in the presence of an angiotensin II infusion (9,10).

Received November 18, 2005. Accepted February 7, 2006.

Published online ahead of print. Publication date available at www.jasn.org.

Address correspondence to: Dr. Dae Ryong Cha, Department of Internal Medicine, Korea University Ansan Hospital, 516 Kojan-Dong, Ansan City, Kyungki-Do, 425-020, Korea. Phone: +82-31-412-6590; Fax: +82-31-412-5574; E-mail: cdragn@unitel.co.kr

Previous reports have demonstrated that administration of spironolactone, a nonselective aldosterone blocker, showed beneficial effects in various animal models of renal injury (11–13). In addition, recent data raise the possibility that inhibition of the aldosterone system may have an additional beneficial effect independent of renin-angiotensin blockade in diabetic nephropathy (14–17). However, it is still unknown whether aldosterone blockade can prevent renal injury through an anti-inflammatory mechanism in this model.

The characteristic features of Otsuka Long-Evans Tokushima Fatty (OLETF) rats, which are the genetic model of type 2 diabetes, are the late onset of hyperglycemia, the chronic course of disease, mild obesity, the clinical onset of diabetes mostly in male rats, and diabetic nephropathy manifested by diffuse glomerulosclerosis and nodular lesions, resembling an advanced stage of human diabetic nephropathy (18,19). These clinical and pathologic characteristics in OLETF rats resemble those of human type 2 diabetes, especially the diabetic nephropathy. Because of these useful characteristics, we performed this experiment using OLETF rats as a type 2 diabetic animal model.

In this study, we investigated the effect of spironolactone on renal function and renal inflammation in the progression of diabetic nephropathy in OLETF rats. In addition, to define the molecular mechanism of spironolactone, we evaluated the effect of aldosterone and spironolactone on the synthesis of

ISSN: 1046-6673/1705-1362

monocyte chemotactic peptide-1 (MCP-1) and determined whether MCP-1 synthesis was mediated *via* the NF-κB pathway in cultured mesangial cells (MC) and proximal tubular cells (PTC).

Materials and Methods

Animal Studies

Male OLETF rats were supplied by the Tokushima Research Institute (Otsuka Pharmaceutical, Otsuka, Japan). Male Long-Evans-Tokushima-Fatty (LETO) rats served as the genetic control for OLETF rats. All rats were kept under controlled temperature (23 ± 2°C) and humidity (55 ± 5%) with an artificial light cycle. The rats were divided into three groups. The first group consisted of LETO rats as controls ($n = 20$). The second group was OLETF rats, which were the type 2 diabetic rats ($n = 20$). The third group was OLETF rats that were treated with 20 mg/kg per d spironolactone (Pharmacia Corp., Peapack, NJ) mixed in food ($n = 20$). This dose of spironolactone is sufficient for blocking the action and specific binding of aldosterone to mineralocorticoid receptors in an *in vivo* kinetic analysis (20). Daily amounts of food intake were checked at regular intervals to affirm the dose of administered drug. Administration of spironolactone was begun at 20 wk of age, which is the time usually required to develop overt hyperglycemia in OLETF rats, and they then were treated for 8 mo. Animals had free access to rat food and were caged individually. Plasma glucose levels were measured using a glucose oxidase–based method, plasma potassium was measured by flame photometry, and serum creatinine levels were determined by a modified Jaffe method. Twenty-four-hour urinary albumin excretion was measured by competitive ELISA (Shibayagi, Shibukawa, Japan). Rats were killed under anesthesia by intraperitoneal injection of sodium pentobarbital 50 mg/kg body wt. At the end of the study period, systolic BP were measured using tail-cuff plethysmography (LE 5001-Pressure Meter; Letica SA, Barcelona, Spain). For observation of serial changes in biochemical parameters, rats were killed before treatment at 8 wk of age, at 20 wk of age, at 1 mo after treatment (24 wk), and 8 mo after treatment (52 wk). Experiments were conducted in accordance with institutional and National Institutes of Health guidelines.

cDNA Microarray Analysis

To identify and study the inflammatory molecules that were down-regulated by spironolactone treatment, we performed cDNA microarray analysis at the end of the study period. Total RNA that were isolated using Trizol reagent from renal cortical tissue were used to synthesize ^{32}P-labeled cDNA by reverse transcription. The general array method used was on the basis of the procedures of DeRisi *et al.* (21). Cluster analysis was performed on Z-transformed microarray data by using two programs that are available as shareware from Michael Eisen's laboratory at Lawrence Berkeley National Laboratories (Berkeley, CA; http://rana.lbl.gov). The clustering of changes in gene expression was determined using a public domain cluster based on a pairwise complete-linkage cluster analysis.

Analysis of Gene Expression by Real-Time Quantitative PCR in Tissues and Cells

Total RNA was extracted from renal cortical tissues or experimental cells with Trizol reagent and purified further using an RNeasy Mini kit (Qiagen, Valencia, CA). Primers were designed from the respective gene sequences using Primer 3 software, and templates' secondary structures were examined and excluded using an *m*-fold software program. Table 1 shows the nucleotide sequence of primers. Quantitative gene expression was performed on a Bio-Rad iCycler system (Bio-Rad, Hercules, CA) using SYBR Green technology. Total mRNA was reverse transcribed into cDNA using an iScript cDNA synthesis kit (Bio-Rad). The real-time reverse transcription–PCR was performed by running for 10 min at 50°C and 5 min at 95°C. Subsequently, 45 cycles that consisting of denaturation for 10 s at 95°C and annealing with extension for 30 s at 60°C were applied. The ratio of each gene and β-actin level (relative gene expression number) was calculated by subtracting the threshold cycle number of the target gene from that of β-actin and raising 2 to the power of this difference.

Determination of MCP-1 Level in Urine and Culture Supernatant

MCP-1 levels were measured by quantitative sandwich ELISA using a commercial kit (Biosource Inc., Camarillo, CA), according to the manufacturer's instructions. The assay was performed in duplicate, and the intensity of the color was measured in an ELISA reader at 450 nm. Urinary MCP-1 levels were expressed relative to the urinary creatinine content and expressed as MCP-1 (pg/mg creatinine), and supernatant MCP-1 levels were expressed relative to the total protein concentration in each condition and expressed as MCP-1 (pg/mg protein).

Table 1. Primer sequences for real-time quantitative PCR[a]

Target gene	Primer Sequence (5′to 3′)	Amplicon Length (bp)
Rat MCP-1, forward	CACCTGCTGCTACTCATTCACT	415
Rat MCP-1, reverse	GTTCTCTGTCATACTGGTCACTTCT	
Rat MIF, forward	GTCACGTAGTCAGGTCCCAG	474
Rat MIF, reverse	CAGCAAGACTCGAAGAACAG	
Rat TGF-β1, forward	ATACAGGGCTTTCGATCCAGG	360
Rat TGF-β1, reverse	GTCCAGGCTCCAAATATAGG	
Rat β-actin, forward	TCATGAGGTAGTCCGTCAGG	460
Rat β-actin, reverse	TCTAGGCACCAAGGTGTG	
Mouse MCP-1, forward	CTGGATCGGAACCAAATGAG	95
Mouse MCP-1, reverse	CGGGTCAACTTCACATTCAA	
Mouse β-actin, forward	GGACTCCTATGTGGGTGACG	118
Mouse β-actin, reverse	CTTCTCCATGTCGTCCCAGT	

[a]MCP-1, monocyte chemotactic peptide-1; MIF, macrophage migration inhibitory factor. In this experiment, each sample was run in triplicate and the corresponding non–reverse-transcribed mRNA sample was used as a negative control. The mRNA level of each sample was normalized to that of β-actin mRNA.

Histologic Examination

The kidney tissues embedded in paraffin were cut into 4-μm-thick slices and were stained with periodic acid-Schiff and Masson trichrome. A semiquantitative score sclerosis index (SI) was used to evaluate the degree of glomerulosclerosis on periodic acid-Schiff–stained sections according to the method described by Ma *et al.* (22). Severity of sclerosis for each glomerulus was graded from 0 to 4+ as follows: 0, no lesion; 1+, sclerosis of <25% of the glomerulus; 2+, sclerosis of 25 to 50%; 3+, sclerosis of >50 to 75%; and 4+, sclerosis of >75%. All histologic examinations were carried out by two pathologists in a blinded manner, and >80 glomeruli were analyzed in kidney sections from each rat.

Immunohistochemical Staining for ED-1, Migration Inhibitory Factor, and TGF-β1

For immunohistochemical staining, renal tissue was sliced in 4-μm sections and placed on microscope slides. For antigen retrieval, specimen slides were transferred to a 10-mmol/L citrate buffer solution (pH 6.0) and then heated at 80°C for 30 min. Then 3.0% H_2O_2/methanol was applied for 20 min to block endogenous peroxidase, and the slides were incubated at room temperature for 20 min with normal goat serum to prevent nonspecific detection. The slides then were incubated for 1 h with primary antibodies against mouse monoclonal anti-monocyte/macrophage (ED-1) antibody (1:100; Serotec, Oxford, UK) or for 2 h with rabbit polyclonal anti–migration inhibitory factor (anti-MIF; 1:20, Zymed Laboratories, San Francisco, CA) and rabbit polyclonal anti–TGF-β1 antibody (1:200; Santa Cruz Biotechnology, Santa Cruz, CA). After rinsing in TBS, slides were incubated in secondary antibody for 30 min. For coloration, slides were incubated with a mixture of 0.05% 3,3′-diaminobenzidine that contained 0.01% H_2O_2 at room temperature, counterstained with Mayer's hematoxylin. Negative control sections were stained under identical conditions with the buffer solution substituting for the primary antibody. We used a NEXES IHC autostainer with an iView 3,3′-diaminobenzidine detection kit (Ventana, Tucson, AZ).

To evaluate immunohistochemical staining for each of the antibodies, we graded glomerular or tubulointerstitial fields semiquantitatively. For ED-1, the numbers of positively stained macrophages were counted under high-power field (×400) in 50 to 60 glomeruli and an average score was calculated and expressed as positive cells/glomerulus. In the tubulointerstitial area, numbers of positively stained macrophage were counted in 10 randomly selected interstitial fields by means of grid fields that measured 0.245 mm^2 and expressed as cells/mm^2. For MIF and TGF-β1, four scores were scaled by extent of positive glomerular and tubulointerstitial field: 0, absent or <25% of the area positive; 1, 25 to 50% of the area positive; 2, 50 to 75% of the area positive; and 3, >75% of the area positive. With regard to MIF staining, most tubules were weakly positive; therefore, we calculated only tubules that showed more than a moderate staining pattern. More than 50 to 60 glomeruli and 10 randomly selected tubulointerstitial fields were evaluated under high-power fields (×400).

Mesangial and Murine Cortical Tubule Cell Cultures

A part of the renal cortex from normal C57BL/6 mice was obtained immediately after surgical nephrectomy, and glomeruli were isolated using differential sieving method. Mesangial cells (MC) were cultured in DMEM supplemented with 17% FCS. Murine cortical tubule (MCT) cells are a cultured line of proximal tubule cells (PTC) that were harvested originally from the renal cortex of SJL mice and functionally characterized by Haverty *et al.* (23) (a gift from Eric G. Neilson, Vanderbilt University, Nashville, TN). The cells were grown in DMEM supplemented with 10% FCS as described previously (23). Subconfluent MC and MCT were serum-starved for 24 h, and various concentrations of aldosterone (Sigma-Aldrich, St. Louis, MO) were added to the culture media at final concentrations of 1, 10, and 100 nM. When the effects of spironolactone (Sigma-Aldrich) were tested, these compounds were added to cells at a concentration of 100 nM 1 hr before aldosterone treatment (100 nM). For evaluation of the effect of NF-κB inhibition on MCP-1 production, NF-κB inhibitor pyrrolidine dithiocarbamate ammonium salt (PDTC; Sigma-Aldrich) was added to cells in some wells at a concentration of 10 μM 30 min before aldosterone treatment (100 nM). All experimental groups were cultured in triplicate and harvested at 24 h for extraction of the total RNA and protein.

Transient Transfection and Luciferase Reporter Activity Assay

A NF-κB reporter plasmid that contained three NF-κB consensus sequences was a gift from Dr. Timothy Blackwell (24). Cells were plated onto 24-well plates at a density of 1×10^5 cells/well. After 24 h of growth, they were transfected with 1 μg of NF-κB reporter plasmid and 1 μg of plasmid that contained Renilla luciferase driven by a TK promotor for 24 h using Superfect (Qiagen, Valencia, CA). Various concentrations of aldosterone were added at final concentrations of 1, 10, and 100 nM. For testing the effects of spironolactone, these compounds were added to cells at a concentration of 100 nM 1 h before aldosterone treatment (100 nM). In some wells, IL-1β was added at a concentration of 2 ng/ml as a positive control. After 24 h, luciferase activity was determined using the dual luciferase assay system according to the manufacturer's instructions (Promega Corp., Madison, WI). For controlling for differences in transfection efficiency, a plasmid that contained Renilla luciferase was included in each transfection and used for normalization.

Extraction of Nuclear Proteins and Western Blotting

Nuclear proteins from cells were extracted using a commercial nuclear extraction kit according to the manufacturer's instructions (Active Motif, Carlsbad, CA). Protein concentration was determined using the bicinchoninic acid method (Pierce Pharmaceuticals, Rockford, IL). Twenty micrograms of protein was electrophoresed on 10% SDS-PAGE mini-gel under denaturing conditions. The proteins were transferred onto a polyvinylidene difluoride membrane (Immobilon-P; Millipore, Bedford, MA) over 150 min at 250 mA. After the membranes were incubated with blocking solution for 1 h at room temperature, the membranes were hybridized with rabbit polyclonal anti-p65 antibody (Santa Cruz Biotechnology) and diluted 1:1000 in blocking buffer overnight at 4°C. The filter then was incubated with horseradish peroxidase–conjugated secondary antibody, diluted 1:1000, for 60 min at room temperature. The detection of specific signals was performed using the ECL method (Amersham, Buckinghamshire, UK). Equal amounts of protein loading were confirmed by β-actin Western staining of the gel.

Statistical Analyses

We used nonparametric analysis because most of the variables, especially the urinary MCP-1, were not normally distributed even after logarithmic transformation. Results were expressed as mean ± SEM. A Kruskall-Wallis test was used for comparison of more than two groups, followed by a Mann-Whitney *U* test for comparison using a microcomputer-assisted program with SPSS for Windows 10.0 (SPSS Inc., Chicago, IL). Correlations between urinary MCP-1 and urinary excretion of albumin were examined by Spearman rank correlation. $P < 0.05$ was considered to be statistically significant.

Results

Biochemical Parameters in Experimental Animals

Table 2 shows the various biochemical results for each group. Kidney/body weight was significantly higher in OLETF rats compared with LETO rats at 20 wk of age. Treatment with spironolactone had no effect on kidney/body weight change and plasma glucose levels. There were no significant differences in serum creatinine concentrations and plasma potassium levels between experimental groups. Systolic BP, measured at the end of the study period, was greater in OLETF rats than in LETO rats, and treatment with spironolactone had no significant effect on systolic BP. Urinary albumin excretion in the OLETF rats was significantly higher than in the LETO rats at 20 wk of age, and the difference gradually increased with the duration of diabetes. Spironolactone treatment significantly reduced urinary albumin excretion throughout the study period. Urinary excretion of MCP-1 did not show any significant differences until 20 wk of age. However, OLETF rats demonstrated significantly higher levels than LETO rats after 24 wk of age. Treatment with spironolactone completely abolished urinary MCP-1 excretion in diabetic OLETF rats. In addition, urinary levels of MCP-1 showed a weak but significant correlation with urinary albumin excretion ($r = 0.163$, $P = 0.015$).

Gene Expression Profiles in OLETF Rats and Spironolactone-Treated Rats

The expression levels of 72 cDNA, which represent 6.25% of the total DNA elements on the array, were changed by more than two-fold in the spironolactone treatment group. The changes ranged from −4.97-fold to 4.07-fold. As shown in Table 3, spironolactone therapy upregulated 17 genes, including several apoptosis-related genes. In contrast, spironolactone treatment downregulated 55 genes, including MCP-1 and MIF.

Histopathologic Changes in Experimental Animals

Figure 1 shows the representative glomerular pathology in the experimental groups at the end of the study period. Using a semiquantitative scoring system, untreated diabetic OLETF rats showed more severe glomerulosclerosis when compared with LETO rats. Spironolactone treatment significantly reduced the glomerulosclerosis, compared with untreated OLETF rats. However, tubulointerstitial fibrosis was not remarkable even in OLETF rats, so significant differences were not found among the three groups.

Expression of MCP-1, MIF, and TGF-β1 in Experimental Animals

MCP-1 mRNA demonstrated a higher level of expression throughout the study period in OLETF rats, compared with LETO rats. In accordance with urinary MCP-1 excretion, MCP-1 gene expression was almost six times higher in the OLETF rats, and the peak level occurred at a relatively early stage of nephropathy (Figure 2A). Similarly, MIF, and TGF-β1 gene expression showed higher levels in the OLETF rats. Spironolactone treatment significantly decreased the gene expression of MCP-1, MIF, and TGF-β1 (Figure 2, B and C).

Representative immunostaining results are shown for ED-1 (Figure 3, A through C), MIF (Figure 3, D through F), and TGF-β1 (Figure 3, G through I). After the onset of diabetes, increased numbers of ED-1–positive monocyte/

Table 2. Biochemical parameters in experimental animals[a]

Time (wk)	Experimental Group	Body Weight (g)	Kidney/Body Weight ($\times 10^{-3}$)	Plasma Glucose (mmol/L)	Plasma K (mmol/L)	Serum Cr (μmol/L)	Urine Volume (ml/d)	Urinary Albumin Excretion (μg/mg Cr per d)	Urinary MCP-1 Excretion (pg/mg Cr per d)	SBP (mmHg)
8	LETO	200.1 ± 6.5	0.31 ± 0.04	8.10 ± 1.85	4.31 ± 0.21	49 ± 11	12.25 ± 6.58	46.54 ± 12.74	21.5 ± 3.72	NA
	OLETF	193.3 ± 6.6	0.32 ± 0.06	6.96 ± 0.38	4.47 ± 0.32	46 ± 12	11.3 ± 0.88	114.76 ± 25.37	20.6 ± 4.02	NA
20	LETO	463.1 ± 25.9	0.29 ± 0.05	9.91 ± 0.22	3.88 ± 0.29	42 ± 9	12.0 ± 2.04	39.99 ± 23.76	28.5 ± 7.39	NA
	OLETF	478.5 ± 23.0	0.41 ± 0.02[b]	13.16 ± 0.62[c]	4.42 ± 0.37	42 ± 10	21.0 ± 1.12[d]	150.01 ± 46.97[e]	23.7 ± 6.12	NA
24	LETO	482.5 ± 25.9	0.30 ± 0.03	9.38 ± 0.13	4.65 ± 0.34	57 ± 14	11.5 ± 3.06	30.41 ± 14.70	28.0 ± 4.23	NA
	OLETF	578.3 ± 20.7	0.39 ± 0.02[b]	21.40 ± 2.49[c]	4.77 ± 0.41	49 ± 13	17.8 ± 6.25[d]	240.69 ± 32.67[e]	59.7 ± 24.21[f]	NA
	OLETF + SPR	581.0 ± 19.5	0.35 ± 0.01[b]	19.54 ± 0.52[c]	4.93 ± 0.51	51 ± 19	15.7 ± 1.95	92.16 ± 37.50[g]	14.8 ± 2.72[h]	NA
52	LETO	590.0 ± 53.6	0.26 ± 0.03	9.23 ± 0.27	4.43 ± 0.29	57 ± 20	11.0 ± 4.14	28.11 ± 11.46	12.4 ± 2.09	101 ± 10
	OLETF	595.8 ± 56.0	0.43 ± 0.04[e]	22.33 ± 2.56[g]	4.88 ± 0.38	47 ± 4	22.5 ± 3.09[d]	497.65 ± 196.4[e]	30.2 ± 6.56[f]	150 ± 14[i]
	OLETF + SPR	568.0 ± 43.9	0.42 ± 0.05[e]	20.99 ± 4.20[c]	5.11 ± 0.43	65 ± 6	19.8 ± 3.16[d]	282.8 ± 107.2[e,g]	11.8 ± 2.93[h]	139 ± 10[i]

[a]Values are expressed as mean ± SEM. Statistical analysis was performed among groups at the same time periods. Cr, creatinine; LETO, Long-Evans-Tokushima-Fatty; NA, not applicable; OLETF, Otsuka Long-Evans Tokushima Fatty; SBP, systolic BP; SPR, spironolactone.

[b]$P < 0.05$, LETO *versus* OLETF and OLETF + SPR.

[c]$P < 0.05$, LETO *versus* OLETF and OLETF + SPR.

[d]$P < 0.05$, LETO *versus* OLETF and OLETF + SPR.

[e]$P < 0.01$, LETO *versus* OLETF and OLETF + SPR.

[f]$P < 0.05$, LETO *versus* OLETF.

[g]$P < 0.01$, OLETF *versus* OLETF + SPR.

[h]$P < 0.05$, OLETF *versus* OLETF + SPR.

[i]$P < 0.05$, LETO *versus* OLETF and OLETF + SPR.

Table 3. Genes regulated by spironolactone treatment in renal cortical tissues[a]

Name of Gene (Fold Change)			
Increased Genes	Decreased Genes		
RAB6, member RAS oncogene family (4.07)	8-oxoguanine DNA glycosylase (−4.97)	Coagulation factor II receptor (−3.40)	Fibroblast growth factor 12 (−2.27)
Expressed sequence tags (3.51)	α2 integrin (−4.84)	Adenosine A2a receptor (−3.27)	Transcription factor 3 (−2.26)
Bruton agammaglobulinemia tyrosine kinase (3.47)	Uroporphyrinogen III synthase (−4.72)	TNF receptor 8 (−3.27)	Tyrosine-tRNA synthase (−2.26)
Membrane co-factor protein (3.28)	IGF 2 (−4.49)	Prostaglandin E receptor 1 (−3.19)	Tropomyosin 4 (−2.25)
S100 calcium-binding protein A10 (3.06)	Interferon receptor 2 (−4.44)	Telomeric repeat binding factor 1 (−2.97)	Death-associated protein (−2.23)
Thioredoxin (3.0)	Small inducible cytokine subfamily A (−4.38)	Complement component 5 receptor (−2.91)	TYRO3 protein tyrosine kinase (−2.19)
Pyrimidinergic receptor P2Y (2.89)	Ubiquitin specific protease 8 −3.95)	Smad 5 (−2.91)	Phosphatase and tensin homolog (−2.17)
RAD51 (*S. cerevisiae*) homolog C (2.69)	v-raf sarcoma viral oncogene B1 (−3.83)	MHC class II DR2 (−2.87)	IL-3 receptor α (−2.14)
Nerve growth factor receptor (2.69)	Colony-stimulating factor 3 receptor (−3.79)	Bcl2-interacting killer (−2.70)	IL-7 (−2.14)
Midkine(neurite growth promoting factor (2.62)	Caspase 9 (−3.76)	Isopentenyl-diphosphate isomerase (−2.69)	Fibroblast growth factor receptor 1 (−2.12)
Caspase 13 (2.61)	v-Ha-ras sarcoma viral oncogene (−3.74)	Solute carrier protein family 11 (−2.65)	Arginine vasopressin receptor 1A (−2.09)
Protein tyrosine phosphatase, receptor type (2.53)	MIF (−3.72)	TNF receptor associated factor 5 (−2.62)	TNF receptor-associated factor 3 (−2.08)
Ribosomal protein L7(2.51)	E2F transcription factor 1 (−3.71)	TNFRSF-interacting kinase 1 (−2.61)	Cerebellin 1 precursor (−2.07)
Menage a trois 1 (CAK assembly factor) (2.50)	Complement component 3a receptor 1 (−3.60)	KIAAO475 gene product (−2.58)	Apoptotic protease activating factor (−2.03)
Nerve growth factor, β polypeptide(2.33)	Deleted in oral cancer 1 (−3.59)	MMP-9 (−2.47)	VEGF (−2.0)
IGF-1 (somatomedic C) (2.06)	TNF receptor 6 (−3.52)	TGF-β-3 (−2.47)	
Tumor protein p53 (2.01)	Guanine nucleotide regulatory protein (−3.51)	Nuclear factor I/X (−2.43)	
	TGF-β–activated kinase-binding protein 1 (−3.48)	Lysosomal deoxyribonuclease II (−2.42)	
	v-abl murine leukemia viral oncogene (−3.47)	YY1 transcription factor (−2.38)	
	α6 integrin (−3.41)	MCP-1 (−2.35)	

[a]cDNA microarray analysis was performed at the end of the study period. Total RNA that were isolated using Trizol reagent from renal cortical tissue then were used to synthesize ^{32}P-labeled cDNA by reverse transcription. Cluster analysis was performed on Z-transformed microarray data. Number in parentheses represents the average fold change compared with control diabetic OLETF rats. MMP, matrix metalloproteinase; VEGF, vascular endothelial growth factor.

macrophages were detected at 24 wk of age in the diabetic kidney and progressively increased according to the duration of diabetes. However, renal macrophage infiltration was rarely detected in LETO rats throughout the study period (Figure 4A). In the diabetic kidney, MIF immunoreactivity was increased primarily in the tubular epithelium, but this was not accompanied by an increase in glomerular MIF expression (Figure 4B). Spironolactone treatment induced significant reductions in both renal ED-1 and MIF protein expression, in accordance with their gene expression. In TGF-β1 immunostaining, diabetic rats exhibited greater immunoreactivity for TGF-β1 in both glomeruli and tubulointerstitium when compared with LETO rats. Spironolactone treatment completely suppressed glomerular TGF-β1 expression (Figure 4C).

Effect of Aldosterone and Spironolactone on MCP-1 Production in Cultured MC and PTC

Aldosterone treatment induced a significant upregulation in MCP-1 gene transcription, and previous treatment with spironolactone abolished this aldosterone-induced MCP-1 expression. In addition, aldosterone increased the release of MCP-1 protein in a dose-dependent manner, and previous treatment with spironolactone abolished aldosterone-induced MCP-1 secretion (Figure 5).

Effect of Aldosterone and Spironolactone on Transcriptional Activity of NF-κB in Cultured MC and PTC

We further evaluated whether MCP-1 production that is induced by aldosterone depends on the NF-κB pathway. We first examined endogenous NF-κB transcriptional activity in

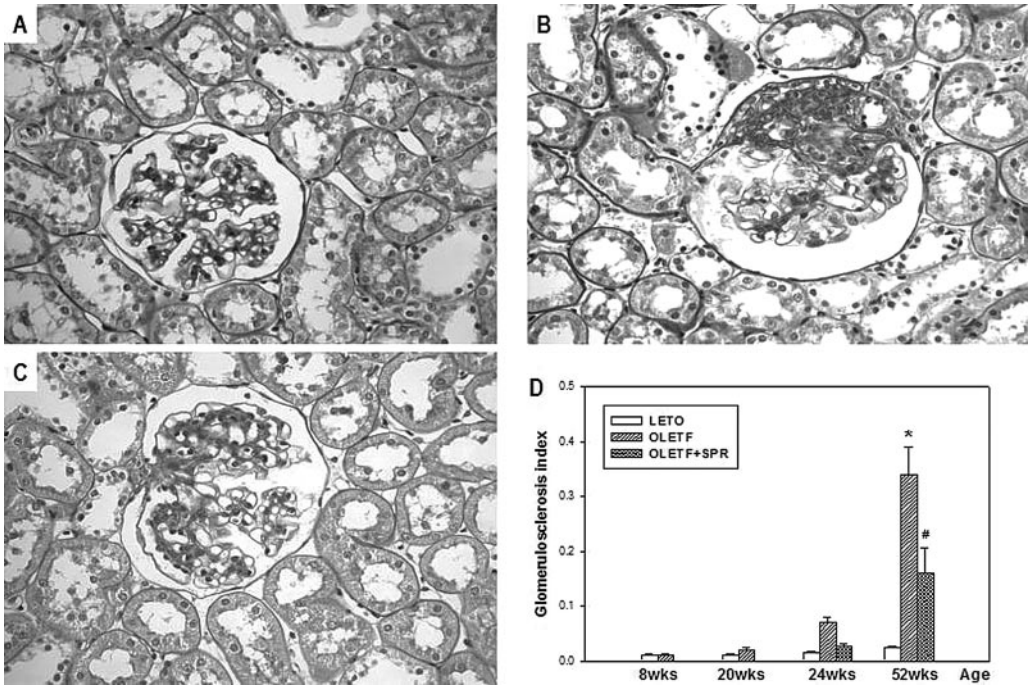

Figure 1. Representative renal histologic findings in experimental animals. (A) Long-Evans-Tokushima-Fatty (LETO) rat at 52 wk of age. (B) Otsuka Long-Evans Tokushima Fatty (OLETF) rat at 52 wk of age. (C) OLETF rat treated with spironolactone (SPR) at 20 mg/kg per d for 8 mo at 52 wk of age. (D) Glomerulosclerosis index in each group, based on the duration of diabetes. Data are mean ± SEM. $^{*}P < 0.05$, LETO *versus* OLETF; $^{\#}P < 0.05$, OLETF *versus* OLETF with SPR. Magnification, ×400; periodic acid-Schiff stain.

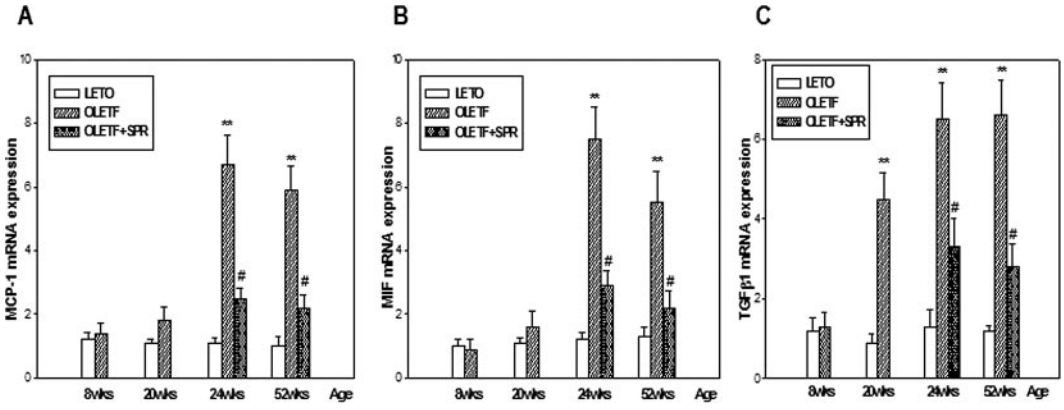

Figure 2. mRNA expression for monocyte chemotactic peptide-1 (MCP-1; A), migration inhibitory factor (MIF; B), and TGF-β1 (C) in experimental groups based on the duration of diabetes. Data are mean ± SEM. $^{**}P < 0.01$, LETO *versus* OLETF; $^{\#}P < 0.05$, OLETF *versus* OLETF with SPR.

cultured cells using a luciferase reporter assay. MC and PTC that were transfected with NF-κB–luciferase exhibited a dose-dependent induction of luciferase activity, but it did not reach statistical significance. Spironolactone treatment significantly suppressed aldosterone-induced NF-κB transcriptional activity (Figure 6, A and B). To confirm further the role of NF-κB activation by aldosterone stimulation, we performed p65 Western blotting using extracted nuclear proteins. As shown in Figure 6C, aldosterone treatment increased nuclear p65 protein expression in both types of cultured cells, which suggests activation of the NF-κB pathway.

Effect of NF-κB Inhibitor on MCP-1 mRNA and Protein Synthesis in Cultured MC and PTC

Because aldosterone increased NF-κB transcriptional activity, we next examined the effect of NF-κB inhibition on MCP-1 synthesis to confirm the role of the NF-κB pathway on MCP-1 production in cultured cells. In both MC and PTC, previous

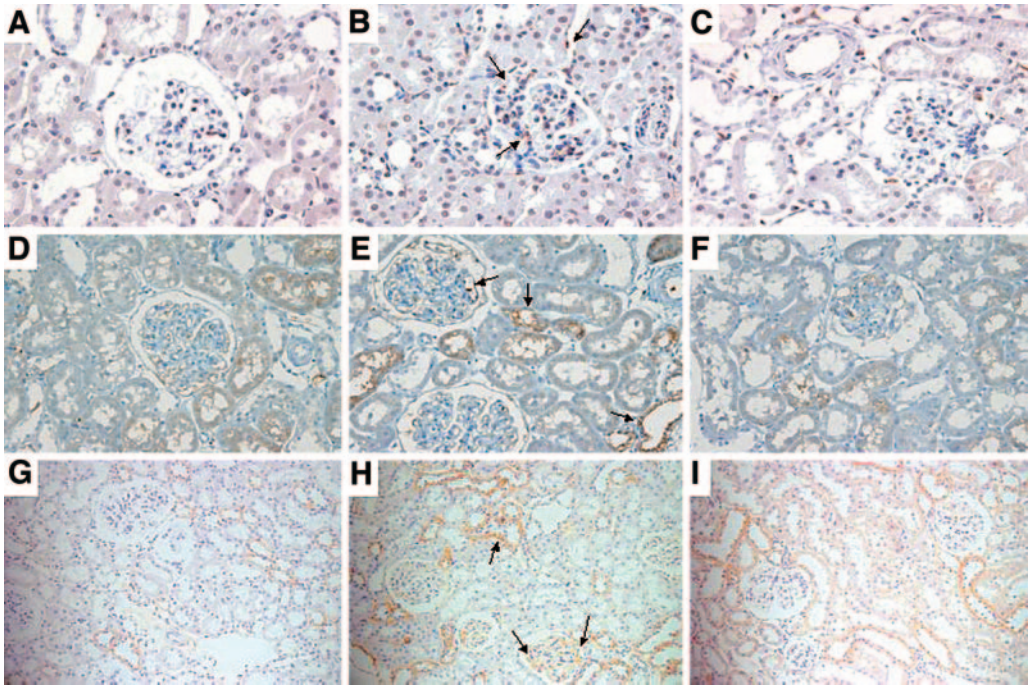

Figure 3. Immunohistochemistry for ED-1, MIF, and TGF-β1 in experimental animals based on the duration of diabetes. Representative immunostained findings at 52 wk of age for ED-1 (A through C), MIF (D through F), and TGF-β1 (G through I). (A, D, and G) LETO rat at 52 wk of age. (B, E, and H) OLETF rat at 52 wk of age. (C, F, and I) OLETF rat treated with SPR at 20 mg/kg per d for 8 mo at 52 wk of age. Positive staining for ED-1, MIF, and TGF-β1 are indicated by short arrows.

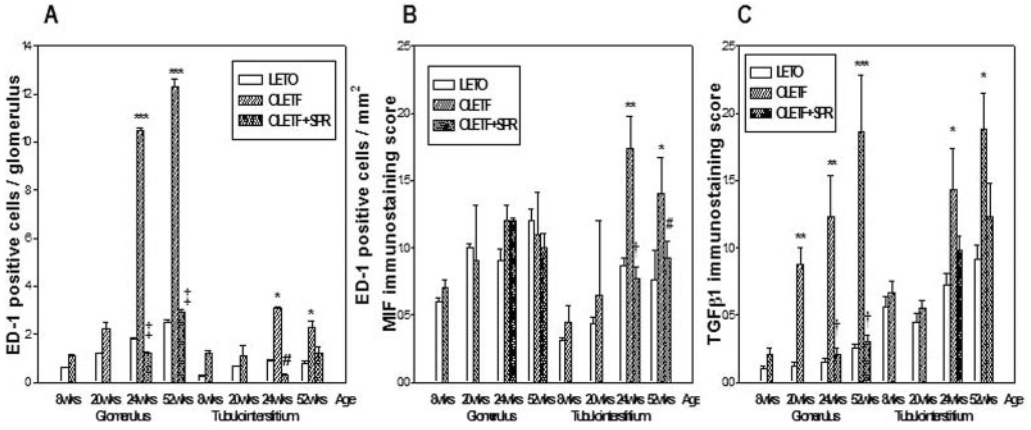

Figure 4. Immunostaining score for ED-1 (A), MIF (B), and TGF-β1 (C) in glomeruli and tubulointerstitial tissues. Data are mean ± SEM. $^{*}P < 0.05$, LETO *versus* OLETF; $^{**}P < 0.01$, LETO *versus* OLETF; $^{***}P < 0.001$, LETO *versus* OLETF; $^{\#}P < 0.05$, OLETF *versus* OLETF with SPR; $^{\dagger}P < 0.01$, OLETF *versus* OLETF with SPR; $^{\ddagger}P < 0.001$, OLETF *versus* OLETF with SPR.

treatment with PDTC, which is a NF-κB inhibitor, abolished aldosterone-induced MCP-1 gene expression (Figure 7A). Furthermore, aldosterone-induced MCP-1 protein secretion was completely suppressed by PDTC treatment (Figure 7B).

Discussion

In this study, we first demonstrated that aldosterone increased MCP-1 synthesis associated with NF-κB activation in MC and PTC. Spironolactone treatment abolished aldosterone-induced MCP-1 synthesis. More important, we have provided evidence that spironolactone treatment decreases urinary albumin excretion and mitigates the glomerulosclerosis that is associated with attenuation of the renal inflammatory process in an animal model of type 2 diabetic nephropathy.

Among the many potential pathogenetic mechanisms that are responsible for the development of diabetic kidney disease, an inflammatory mechanism has been suggested to play a role in the development of diabetic nephropathy (25–27). Urinary MCP-1 excretion increases in patients with early diabetic nephropathy, and acute-phase markers of inflammation are asso-

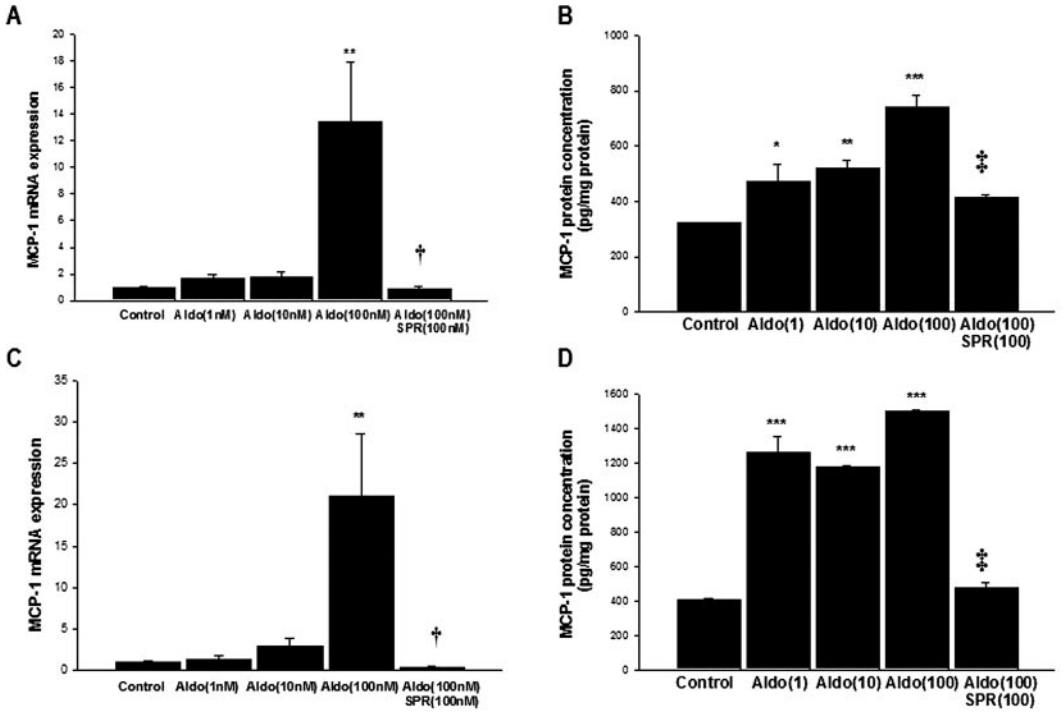

Figure 5. Effect of various concentrations of aldosterone on MCP-1 mRNA expression and protein production in cultured mesangial cells (MC; A and B) and proximal tubule cells (PTC; C and D). Data are mean ± SEM. Aldo, aldosterone; $^{*}P < 0.05$, control *versus* aldosterone; $^{**}P < 0.01$, control *versus* Aldo; $^{***}P < 0.001$, control *versus* Aldo; $^{\dagger}P < 0.01$, Aldo *versus* Aldo with SPR; $^{\ddagger}P < 0.001$, Aldo *versus* Aldo with SPR.

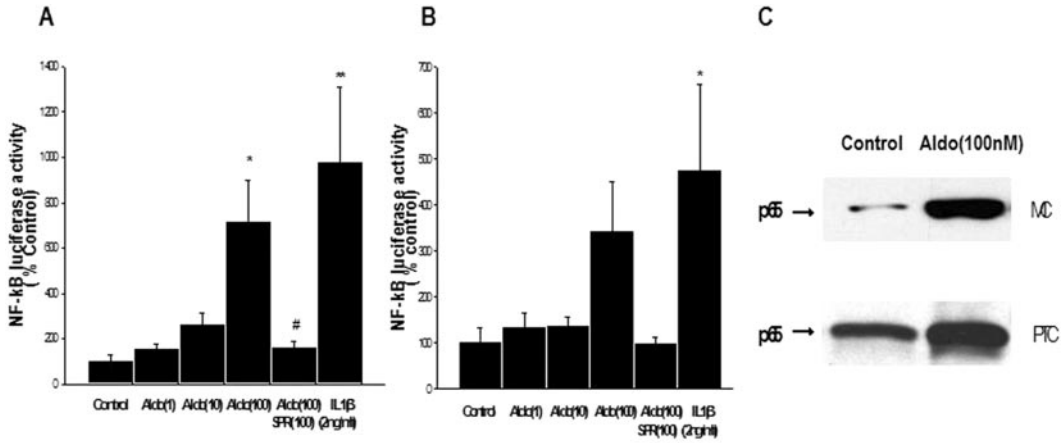

Figure 6. Effect of Aldo on NF-κB activity in cultured MC and PTC. MC (A) and PTC (B) were co-transfected with NF-κB promotor-driven luciferase vector and a TK driving Renilla luciferase plasmid. Then cells were treated with Aldo at concentrations of 1, 10, or 100 nM for 24 h. SPR was added to cells at a concentration of 100 nM 1 h before Aldo treatment (100 nM). NF-κB reporter activity was normalized to Renilla luciferase activity. (C) Representative immunoblot using nuclear protein from cultured cells for NF-κB p65. Data are mean ± SEM. $^{*}P < 0.05$, control *versus* Aldo and IL-1β; $^{**}P < 0.01$, control *versus* Aldo and IL-1β; $^{\#}P < 0.05$, Also *versus* Aldo with SPR.

ciated with the nephropathy state in patients with type 2 diabetes (25,26).

In this study, we found that spironolactone treatment downregulated many of the genes that are involved in the inflammatory process, such as MCP-1, MIF, the TNF receptor, and IL and its receptor. In addition, spironolactone decreased the matrix-regulating gene expression, including TGF-β, matrix metalloproteinase, IGF, and vascular endothelial growth factor. To confirm further the microarray data, we observed changes in representative inflammatory molecules, including MCP-1 and MIF. We observed that MCP-1 gene expression and urinary excretion of the protein were concurrently increased at 24 wk of age, after the onset of hyperglycemia. We also noted that ED-1–positive cells accumulate in the diabetic kidney at the same

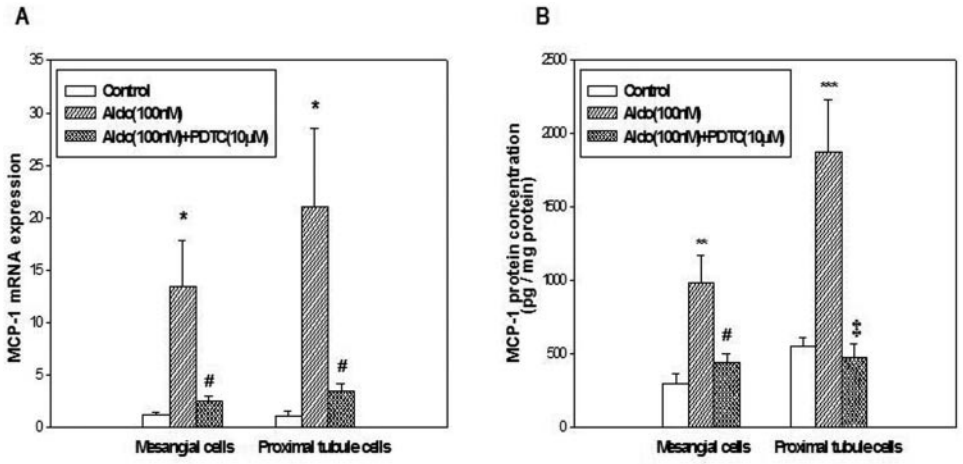

Figure 7. Effect of NF-κB inhibitor pyrrolidine dithiocarbamate (PDTC) on MCP-1 mRNA expression (A) and MCP-1 protein synthesis (B) in cultured MC and PTC. Cells were treated with Aldo at a concentration of 100 nM for 24 h. PDTC was added to cells at a concentration of 10 μM 1 h before Aldo treatment (100 nM). Data are mean ± SEM. $^{*}P < 0.05$, control *versus* Aldo; $^{**}P < 0.01$, control *versus* Aldo; $^{***}P < 0.001$, control *versus* Aldo; $^{\#}P < 0.05$, Aldo *versus* Aldo with PDTC; $^{\ddagger}P < 0.001$, Aldo *versus* Aldo with PDTC.

time. In addition, MIF gene expression increased at approximately 24 wk of age. Although we could not find significant changes in MIF expression in the diabetic glomeruli, MIF expression was markedly increased in the tubular epithelium of the diabetic kidney. In agreement with a previous report (28), MIF protein was localized primarily to tubular epithelial cells in both control and diabetic rats.

However, the exact role of MIF in the pathogenesis of diabetic nephropathy still is unknown. MIF inhibits migration of macrophage from tissues and has an important position at the pinnacle of the inflammatory cascade. There is considerable experimental evidence that MIF is closely related to macrophage accumulation and renal injury. Renal MIF expression is upregulated in proliferative forms of glomerulonephritis, and angiotensin II treatment upregulates MIF production in cultured tubular epithelial cells (29–31).

Although previous reports have demonstrated the beneficial effect of spironolactone in various animal models of renal injury, little *in vivo* evidence is available on the potential mechanism of aldosterone blockade in type 2 diabetic nephropathy. Aldosterone escape during long-term blockade of the renin-angiotensin system is associated with an enhanced decline in GFR in patients with type 1 diabetes and nephropathy, and aldosterone inhibition has an additional renal protective effect for patients who have early diabetic nephropathy and have the aldosterone escape phenomenon during angiotensin-converting enzyme inhibitor treatment (17,32,33).

In this study, we observed that spironolactone therapy significantly reduced urinary albumin excretion, even after 1 mo of treatment, without affecting blood glucose concentration, systolic BP, and kidney-to-body weight ratios in diabetic rats. This suggests that the beneficial effect of spironolactone is independent of both hemodynamic and metabolic mechanisms. We also noted that the plasma potassium concentration was slightly higher in the diabetic rats and that spironolactone treatment did not induce a significant elevation in plasma potassium levels. Spironolactone treatment abolished urinary levels of MCP-1 excretion that are associated with a reduction in renal MCP-1 gene expression and abolished macrophage accumulation in the diabetic kidney. Furthermore, we noted that spironolactone treatment markedly suppressed the expression of TGF-β1 in the diabetic kidney, and mitigation of the effects of these molecules by spironolactone suggests that aldosterone may contribute to overproduction of TGF-β1 in the diabetic kidney. In support of the role of aldosterone in the regulation of TGF-β1, Juknevicius *et al.* (34) recently reported that systemic aldosterone administration provokes renal TGF-β synthesis in normal rats and suggest that aldosterone may contribute to renal fibrosis through this mechanism. In our experiment, we did not measure the aldosterone level in the diabetic kidney, and it is not clear whether aldosterone synthesis is actually increased in this circumstance. However, that mesangial cells produce aldosterone in response to LDL and angiotensin II suggests the possibility that renal aldosterone synthesis may be increased in the diabetic kidney (35).

In this study, we observed that aldosterone treatment induced a marked upregulation of MCP-1 synthesis, and spironolactone treatment abolished this aldosterone-induced MCP-1 production in intrinsic renal cells. This finding agrees with *in vivo* results that showed inhibition of urinary excretion of MCP-1 and renal MCP-1 synthesis in spironolactone-treated diabetic rats. This is supported by a recent report that showed that systemic administration of aldosterone induced macrophage infiltration and upregulation of MCP-1 and that treatment with eplerenone attenuates MCP-1 expression and macrophage infiltration in experimental rats (36).

In the past decade, several studies have revealed that a mineralocorticoid receptor is involved in NF-κB activation (37,38). Sun *et al.* (8) reported that aldosterone-induced MCP-1 expression was mediated by NF-κB in cardiac tissues. How-

ever, it is not clear which mechanism is involved in aldosterone-induced MCP-1 stimulation in renal tissue. In this study, we provide evidence that aldosterone-induced NF-κB activation is followed by MCP-1 synthesis in cultured renal cells. Aldosterone induced increases in the transcriptional activity of NF-κB, and previous treatment with spironolactone abolished aldosterone-induced NF-κB transcriptional activity. Furthermore, treatment with NF-κB inhibitor abolished aldosterone-induced MCP-1 overproduction. To the best of our knowledge, these results are the first to show that aldosterone receptor blockade has a renal protective effect *via* an anti-inflammatory mechanism in experimental type 2 diabetic kidney.

The limitation of this study is that we measured BP only at the end of the study period, so we cannot exclude the possibility that the BP was lower at any time during the study period in the spironolactone-treated group. Additional hemodynamic factors as well as nonhemodynamic ones may be operative in producing a beneficial effect of spironolactone treatment.

Conclusion

This study suggests that aldosterone induces MCP-1 overproduction *via* transcriptional activation of the NF-κB pathway in intrinsic renal cells and that spironolactone treatment inhibits this NF-κB activation and MCP-1 production. Spironolactone therapy also showed renal protective effects associated with a decrease in the renal inflammatory process. Therefore, aldosterone receptor blockade may be an additional therapeutic target for limiting the progression of diabetic nephropathy.

Acknowledgments

This work was supported by grant R01-2002-000-00139-0 from the Basic Research Program of the Korea Science & Engineering Foundation.

We thank Professor Eric G. Neilson for the generous gift of the mouse MCT cell line and Tokushima Research Institute, Otsuka Pharmaceutical Co., Ltd., for provision of OLETF rats.

References

1. Banba N, Nakamura T, Matsumura M, Kuroda H, Hattori Y, Kasai K: Possible relationship of monocyte chemoattractant protein-1 with diabetic nephropathy. *Kidney Int* 58: 684–690, 2000
2. Sassy-Prigent C, Heudes D, Mandet C, Belair MF, Michel O, Perdereau B, Bariety J, Bruneval P: Early glomerular macrophage recruitment in streptozotocin-induced diabetic rats. *Diabetes* 49: 466–475, 2000
3. Schneider A, Panzer U, Zahner G, Wenzel U, Wolf G, Thaiss F, Helmchen U, Stahl RA: Monocyte chemo-attractant protein-1 mediates collagen deposition in experimental glomerulonephritis by transforming growth factor-beta. *Kidney Int* 56: 135–144, 1999
4. Utimura R, Fujihara CK, Mattar AL, Malheiros DM, De Lourdes Noronha I, Zatz R: Mycophenolate mofetil prevents the development of glomerular injury in experimental diabetes. *Kidney Int* 63: 209–216, 2003
5. Han SY, So GA, Jee YH, Han KH, Kang YS, Kim HK, Kang SW, Han DS, Han JY, Cha DR: Effect of retinoic acid in experimental diabetic nephropathy. *Immunol Cell Biol* 82: 568–576, 2004
6. Chow F, Ozols E, Nikolic-Paterson DJ, Atkins RC, Tesch GH: Macrophages in mouse type 2 diabetic nephropathy: Correlation with diabetic state and progressive renal injury. *Kidney Int* 65: 116–128, 2004
7. Rocha R, Rudolph AE, Frierdich GE, Nachowiak DA, Kekec BK, Blomme EA, McMahon EG, Delyani JA: Aldosterone induces a vascular inflammatory phenotype in the rat heart. *Am J Physiol Heart Circ Physiol* 283: H1802–H1810, 2002
8. Sun Y, Zhang J, Lu L, Chen SS, Quinn MT, Weber KT: Aldosterone-induced inflammation in the rat heart: Role of oxidative stress. *Am J Pathol* 161: 1773–1781, 2002
9. Rocha R, Chander PN, Zuckerman A, Stier CT Jr: Role of aldosterone in renal vascular injury in stroke-prone hypertensive rats. *Hypertension* 33: 232–237, 1999
10. Rocha R, Stier CT Jr, Kifor I, Ochoa-Maya MR, Rennke HG, Williams GH, Adler GK: Aldosterone: A mediator of myocardial necrosis and renal arteriopathy. *Endocrinology* 141: 3871–3878, 2000
11. Trachtman H, Weiser AC, Valderrama E, Morgado M, Palmer LS: Prevention of renal fibrosis by spironolactone in mice with complete unilateral ureteral obstruction. *J Urol* 172[Suppl 4]: S1590–S1594, 2004
12. Feria I, Pichardo I, Juarez P, Ramirez V, Gonzalez MA, Uribe N, Garcia-Torres R, Lopez CF, Gamba G, Bobadilla NA: Therapeutic benefit of spironolactone in experimental cyclosporine A nephrotoxicity. *Kidney Int* 63: 43–52, 2003
13. Blasi ER, Rocha R, Rudolph AE, Blomme EAG, Polly ML, McMahon EG: Aldosterone/salt induces renal inflammation and fibrosis in hypertensive rats. *Kidney Int* 63: 1791–1800, 2003
14. Fujisawa G, Okada K, Muto S, Fujita N, Itabashi N, Kusano E, Ishibashi S: Spironolactone prevents early renal injury in streptozotocin-induced diabetic rats. *Kidney Int* 66: 1493–1502, 2004
15. Miric G, Dallemagne C, Endre Z: Reversal of cardiac and renal fibrosis by pirfenidine and spironolactone in streptozotocin-diabetic rats. *Br J Pharmacol* 133: 687–694, 2001
16. Nitta K, Uchida K, Nihei H: Spironolactone and angiotensin receptor blocker in nondiabetic renal diseases. *Am J Med* 117: 444–445, 2004
17. Sato A, Hayashi K, Naruse M, Saruta T: Effectiveness of aldosterone blockade in patients with diabetic nephropathy. *Hypertension* 41: 64–68, 2003
18. Kawano K, Hirashima T, Mori S, Saitoh Y, Kurosumi M, Natori T: Spontaneous long-term hyperglycemic rat with diabetic complications. Otsuka Long-Evans Tokushima Fatty (OLETF) strain. *Diabetes* 41: 1422–1428, 1992
19. Kawano K, Mori S, Hirashima T, Man ZW, Natori T: Examination of the pathogenesis of diabetic nephropathy in OLETF rats. *J Vet Med Sci* 61: 1219–1228, 1999
20. de Gasparo M, Joss U, Ramjoue HP, Whitebread SE, Haenni H, Schenkel L, Kraehenbuehl C, Biollaz M, Grob J, Schmidlin J: Three new epoxy-spironolactone derivatives: Characterization in vivo and in vitro. *J Pharmacol Exp Ther* 240: 650–656, 1987
21. DeRisi J, Penland L, Brown PO, Bittner ML, Meltzer PS, Ray M, Chen Y, Su YA Trent JM: Use of a cDNA microarray to analyse gene expression patterns in human cancer. *Nat Genet* 14: 457–460, 1996

22. Ma LJ, Nakamura S, Aldigier JC, Rossini M, Yang H, Liang X, Nakamura I, Marcantoni C, Fogo A: Regression of glomerulosclerosis with high-dose angiotensin inhibition is linked to decreased plasminogen activator inhibitor-1. *J Am Soc Nephrol* 16: 966–976, 2005
23. Haverty TP, Kelly CJ, Hines WH, Amenta PS, Watanabe M, Harper RA, Kefalides NA, Neilson EG: Characterization of a renal tubular epithelial cell line which secretes the autologous target antigen of autoimmune experimental interstitial nephritis. *J Cell Biol* 107: 1359–1368, 1988
24. Blackwell TS, Yull FE, Chen CL, Venkatakrishnan A, Blackwell TR, Hicks DJ, Lancaster LH, Christman JW, Kerr LD: Use of genetically altered mice to investigate the role of nuclear factor-kappa B activation and cytokine gene expression in sepsis-induced ARDS. *Chest* 116[Suppl 1]: S73–S74, 1999
25. Wada T, Furuichi K, Sakai N, Iwata Y, Yoshimoto K, Shimizu M, Takeda SI, Takasawa K, Yoshimura M, Kida H, Kobayashi KI, Mukaida N, Naito T, Matsushima K, Yokoyama H: Up-regulation of monocyte chemo-attractant protein-1 in tubulo-interstitial lesions of human diabetic nephropathy. *Kidney Int* 58: 1492–1499, 2000
26. Dalla Vestra M, Mussap M, Gallina P, Bruseghin M, Cernigoi AM, Saller A, Plebani M, Fioretto P: Acute-phase markers of inflammation and glomerular structure in patients with type 2 diabetes. *J Am Soc Nephrol* 16[Suppl 1]: S78–S82, 2005
27. Kikuchi Y, Imakiire T, Yamada M, Saigusa T, Hyodo T, Hyodo N, Suzuki S, Miura S: Mizoribine reduces renal injury and macrophage infiltration in non-insulin dependent diabetic rats. *Nephrol Dial Transplant* 20: 1573–1581, 2005
28. Lan HY, Yang N, Nikolic-Paterson DJ, Yu XQ, Mu W, Isbel NM, Metz CN, Bucala R, Atkins RC: Expression of macrophage migration inhibitory factor in human glomerulonephritis. *Kidney Int* 57: 499–509, 2000
29. Lan HY, Yang N, Metz C, Mu W, Song Q, Nikolic-Paterson DJ, Bacher M, Bucala R, Atkins RC: TNF-alpha up-regulates renal MIF expression in rat crescentic glomerulonephritis. *Mol Med* 3: 136–144, 1997
30. Lan HY, Bacher M, Yang N, Mu W, Nikolic-Paterson DJ, Metz C, Meinhardt A, Bucala R, Atkins RC: The pathogenic role of macrophage migration inhibitory factor in immunologically induced kidney disease in the rat. *J Exp Med* 185: 1455–1465, 1997
31. Rice EK, Tesch GH, Cao Z, Cooper ME, Metz CN, Bucala R, Atkins RC, Nikolic-Paterson DJ: Induction of MIF synthesis and secretion by tubular epithelial cells: A novel action of angiotensin II. *Kidney Int* 63: 1265–1275, 2003
32. Schjoedt KJ, Anderson S, Rossing P, Tarnow L, Parving HH: Aldosterone escape during blockade of the renninangiotensin-aldosterone system in diabetic nephropathy is associated with enhanced decline in glomerular filtration rate. *Diabetologia* 47: 1936–1939, 2004
33. Sato A, Hayashi K, Saruta T: Antiproteinuric effects of mineralocorticoid receptor blockade in patients with chronic renal disease. *Am J Hypertens* 18: 44–49, 2005
34. Juknevicius I, Segal Y, Kren S, Lee R, Hostetter TH: Effect of aldosterone on renal transforming growth factor-beta. *Am J Physiol Renal Physiol* 286: F1059–F1062, 2004
35. Nishikawa T, Suematsu S, Saito J, Soyama A, Ito H, Kino T, Chrousos G: Human mesangial cells produce aldosterone in response to low density lipoprotein (LDL). *J Steroid Biochem Mol Biol* 96: 309–316, 2005
36. Rocha R, Rudolph AE, Frierdich GE, Nachowiak DA, Kekec BK, Blomme EAG, Mcmahon EG, Delyani JA: Aldosterone induces a vascular inflammatory phenotype in the rat heart. *Am J Physiol Heart Circ Physiol* 283: H1802–H1810, 2002
37. Fiebeler A, Schmidt F, Muller DN, Park JK, Dechend R, Bieringer M, Shagdarsuren E, Breu V, Haller H, Luft FC: Mineralocorticoid receptor affects AP-1 and nuclear factor-kappaB activation in angiotensin II-induced cardiac injury. *Hypertension* 37: 787–793, 2001
38. Kolla V, Litwack G: Inhibition of mineralocorticoid-mediated transcription by NF-kappaB. *Arch Biochem Biophys* 383: 38–45, 2000